Shariati *et al. Microbial Cell Factories* (2024) 23:318
https://doi.org/10.1186/s12934-024-02587-8

Microbial Cell Factories

RESEARCH Open Access

Optimized production of a truncated form of the recombinant neuraminidase of influenza virus in *Escherichia coli* as host with suitable functional activity

Fatemeh Sadat Shariati[1], Fatemeh Fotouhi[1*], Behrokh Farahmand[1], Zahra Barghi[1] and Kayhan Azadmanesh[2*]

Abstract

Background To discover effective drugs for treating Influenza (a disease with high annual mortality), large amounts of recombinant neuraminidase (NA) with suitable catalytic activity are needed. However, the functional activity of the full-length form of this enzyme in the bacterial host (as producing cells with a low cost) in a soluble form is limited. Thus, in the present study, a truncated form of the neuraminidase (derived from California H1N1 influenza strain) was designed, then biosynthesized in *Escherichia coli* BL21 (DE3), Shuffle T7, and SILEX systems. *E. coli* BL21 (DE3) was selected as a best host for statistical optimization. Using central composite design methodology, neuraminidase expression level was measured at 20 different runs considering most effective factors including; concentration of isopropyl-β-D-thiogalactopyranoside (IPTG), temperature, and induction time.

Result The recombinant neuraminidase was purified using Ni-affinity chromatography in soluble form. The neuraminidase expression was confirmed by western blot technique with a molecular mass of 48 kDa. The optimum expression condition was at temperature (30°C), induction time (3 h), and concentration of IPTG (0.6 mM) resulting in maximum neuraminidase expression (7.6 µg/mL) with $P < 0.05$. The analysis of variance with the significant value of R^2 (0.97) indicated that the quadratic model utilized for this prediction was highly significant ($p < 0.0001$). Applying the optimized condition led to a ~ 2.2-fold increase in NA expression level (from 3.4 to 7.6 µg/ml). The kinetic parameters were also confirmed by fluorescent signals (by 2′-(4-Methylumbelliferyl)-α-D-N acetyl neuraminic acid substrate) with specific activity; ~3.5 IU/mg and Km: 86.49 ± 0.1 µ, close to the *Vibrio Cholera* neuraminidase with specific activity; 4 IU/mg. The neuraminidase inhibition test confirmed the inhibition of the neuraminidase activity by the drug inhibitor (Oseltamivir) compared to the control sample.

Conclusion The high quality and proper functional activity of the truncated neuraminidase described in this research show that *E. coli* can be a suitable host for a wide range of applications with less cost and risk compared to eukaryotic expression systems.

*Correspondence:
Fatemeh Fotouhi
fotouhi@pasteur.ac.ir
Kayhan Azadmanesh
azadmanesh@pasteur.ac.ir

Full list of author information is available at the end of the article

© The Author(s) 2024. **Open Access** This article is licensed under a Creative Commons Attribution-NonCommercial-NoDerivatives 4.0 International License, which permits any non-commercial use, sharing, distribution and reproduction in any medium or format, as long as you give appropriate credit to the original author(s) and the source, provide a link to the Creative Commons licence, and indicate if you modified the licensed material. You do not have permission under this licence to share adapted material derived from this article or parts of it. The images or other third party material in this article are included in the article's Creative Commons licence, unless indicated otherwise in a credit line to the material. If material is not included in the article's Creative Commons licence and your intended use is not permitted by statutory regulation or exceeds the permitted use, you will need to obtain permission directly from the copyright holder. To view a copy of this licence, visit http://creativecommons.org/licenses/by-nc-nd/4.0/.

Keywords Truncated neuraminidase, Influenza virus H1N1, Soluble neuraminidase expression, Central composite design, SILEX systems

Introduction

Influenza virus creates severe epidemics of respiratory disease with high annual morbidity and mortality (an estimation of 250000–500000 million cases) [1]. The importance of influenza in the spread of disease between people is due to antigen shift [2], the speed of the spread [3], the extent and number of patients, and the severity of its complications. Vaccination is the suitable and effective solution to prevent and control influenza. In addition to vaccination, the use of NA inhibitors (NAI) [3, 4] is one of the best methods for treating influenza disease by inhibition of release of influenza viruses from host cells [5–8]. The research indicated that the resistance of viruses against the pharmacological inhibitors of NA has enhanced. Since, a high amount of biologically active NA with low cost is required to be used in the laboratory environment to discover new drugs that inhibit the neuraminidase activity of this enzyme [4, 9]. However, there are limitations in the extraction of native form or the recombinant expression of this enzyme in eukaryotic and prokaryotic hosts, which are described below.

NA is tetrameric membrane proteins that its sialidase activity leads to the release of new virus particles from infected cells. The native extraction process of NA includes disadvantages [5, 10, 11] of: (i) the high risk and possible spread of the live virus, (ii) the need for special laboratory equipment, (iii) obtaining a small amount of the enzyme, and (iv) a long time for the production of enzyme [1, 12, 13]. Moreover, based on the results of previous studies, it can be concluded that the expression of this enzyme in eukaryotic cells is associated with disadvantages such as: (i) hyper glycosylation of recombinant proteins, (ii) changes in their catalytic properties, (iii) high cost, (iv) long production time, (v) low stability, (vi) and low protein yield [14, 15]. Currently, eukaryotic expression systems such as yeast, plants, insect, and animal cells are widely used to produce recombinant NA enzymes. For example, in a study by Campbell et al., the expression of H1N1 NA was investigated in the eukaryotic host HEK293-6E [14]. In the yeast host, the expressed NA has demonstrated hyperglycosylation, which results in the expression of NA with high molecular weight compared with the NA produced on the surface of virus-infected human cells. The expression of NA in tobacco plants leads to an insoluble product [16, 17]. The baculovirus/insect cell expression systems are successful in producing large amounts of soluble and active NA, at the same time, the survival and maintenance of these expression systems have limitations [17–19]. Also, in a study conducted by Lipnicanova et al., the result showed that the expression of full-length NA enzyme in the *E. coli* BL21 (DE3) pLysS, and Arctic Express (DE3) host (as a host with low cost) lead to the formation of inclusion bodies. The aggregation of NA imposes a high cost on the system due to lengthy processes for purification and refolding. Moreover, enzymatic properties decrease due to improper folding [20].

The NA enzyme consists of a tetramer of four identical polypeptides. Each monomer folds into four distinct structural domains: the cytoplasmic tail, the transmembrane part, the stalk, and the head of the enzyme [5]. The presence of trans membrane region (hydrophobic domain) in the expression of recombinant proteins in eukaryotic hosts plays an effective role in the formation of inclusions bodies. Therefore, in the present study, to produce the functional and soluble form of the NA enzyme in the bacterial host, the NA was truncated based on bioinformatics studies for bypassing mentioned limitations. The studies showed that the active site of the NA is located in the head domain of the enzyme. The parts of the stalk that are adjacent to the head of the enzyme, play a prominent role in the stability of the enzyme.

The expression of the truncated form of NA optimized at *E. coli* BL21 (DE3), Hsp27/Hsp40 SILEX systems, and Shuffle T7 (It is a bacterial host with good ability to form disulfide bond of recombinant protein) [21, 22]. To further optimize the culture conditions, the host with the highest expression level of NA enzyme was selected. Central composite design (CCD) method was utilized for the optimization of NA expression in *E. coli* BL21 (DE3) system at 5-level using three parameters (temperature, induction time, and the concentration of IPTG). This statistical approach helps us achieve the optimum expression condition of NA with a small number of experiments compared to a full factorial [23]. Then, the overexpressed recombinant NA protein was purified for subsequent biochemical characterizations. The results of the kinetic parameters of the NA were measured in optimized conditions, and compared to functional activity of the commercial sample.

Methods and materials

Designing the truncated form of NA

A DNA sequence encoding the full-length of neuraminidase (influenza A virus /California/07/2009 (H1N1)) with Uniprot ID: C3W6G3_9INFA was selected (8 disulfide bond and without glycosylation site) based on BLAST results, the absence of glycosylation site, identification of domains for different subtypes of influenza virus, as well as previous laboratory studies. To identify conserved

regions in the NA, the full-length NA sequence and its head domain (at different subtypes of influenza) were blasted separately. The Uniprot database studies showed that the NA is a tetramer enzyme, and the active site of the enzyme is located in the head site of the enzyme (91–469 aa) with ~99.5% similarity (in H1N1 subtypes). The sequences 1–7 aa, 7–34 aa, and 34–91 aa are related to the tail, transmembrane, and stalk domain, respectively. Finally, the NA gene of influenza A virus /California/07/2009 (H1N1) was truncated by removing of the cytoplasmic domain, transmembrane region, and parts of the stalk. For proper folding of the NA enzyme, the cysteine sequence was preserved in the stalk of the enzyme. Also, previous studies show that the addition of the tag does not affect the enzymatic activity of the enzyme at near of the head site. Therefore, in this study, truncation was not performed near the head site of the enzyme [5, 24, 25].

Bacterial strains, plasmids, and growth condition

The truncated form of NA gene was codon optimized, and synthesized by Poreteogenix company (France). *hsp27* (P04792) and *hsp40* (P25685) coding sequences were synthesized for autoinduction of the SILEX system in *E. coli* BL21 (DE3) host according to our previous study [21]. *E. coli* BL21 (DE3) and Shuffle T7 strains were used for the expression of the NA enzyme. All strains were achieved from the Pasteur Institute of Iran. The NA gene was cloned into pET28a using *Xba* I and *Xho*I restriction sites to construct pET28a-*na*. Plasmids were transformed into *E. coli* BL21 (DE3) and Shuffle T7 with the heat-shock method [21]. Bacterial cells were grown in Luria Bertani broth (LB) (10 g/L tryptone, 5 g/L yeast extract and 10 g/L sodium chloride) and Super Optimal Broth (SOB) (5 g/L yeast extract, 20 g/L tryptone, and 0.5 g/L sodium chloride) medium supplemented with antibiotics; 50 µg/ml kanamycin and 25 µg /mL spectinomycin [26], respectively. Moreover, the expression of NA enzyme was investigated by Hsp27 and Hsp40 SILEX systems according to our previous studies [21, 22].

NA expression analysis with Western blot in bacterial host

To optimize the expression of the NA enzyme, several different hosts, *E. coli* Bl21(DE3), Shuffle T7, and (Hsp27 and Hsp40) SILEX systems were selected, and the protein expression was measured at two temperatures of 29 °C and 37 °C, three different concentrations of IPTG inducer (0.1, 0.5 and 1 mM IPTG was added at OD_{600nm} ~ 0.6), and induction time 2, 3, 4 and 16 h. Briefly, a single clone was selected, and inoculated into 5 mL of LB medium. The medium containing bacteria was incubated for 16 h at 37°C/180 rpm. Then, 100 µL of overnight bacterial culture was added to a 5 mL LB medium, and incubated for another 16 h at 29°C/180 rpm. One milliliter of culture medium containing the expressed NA were collected at intervals of 2, 3, 4 and 16 h, and centrifuged for 10 min at 9000 *g*. The bacterial pellet was resuspended in a mixture of 5x sample loading (100 µL) containing 2-mercaptoethanol (5%), 0.004% bromophenol blue, 10% SDS, and 50 mM phosphate buffer at pH 7.0, and boiled for 10 min at 100˚C. The NA expression was evaluated using of 12% gel SDS-PAGE, and staining with Coomassie blue. Also, the NA expression level was measured by the intensity of the protein bands on SDS-PAGE gel using Image J software (https://imagej.nih.gov/ij/index.html) [27].

Based on the reported results, the host with the highest NA expression (*E. coli* BL21 (DE3)) was selected for further optimization the culture conditions using Design-Expert software [28–30]. After of SDS-PAGE process, the samples of NA expressed in *E. coli* BL21 (DE3) were transferred with a Transfer buffer (glycine 96 mM, Tris 12.5 mM pH: 8.3, and methanol 10% (V/V)) on nitrocellulose membrane for 20 min (Sigma-Aldrich, USA), and blocked in distilled water containing 2.5% BSA for 16 h at 4 °C. A buffer containing anti-His Tag antibody (Sigma- Aldrich, USA) was added to the membrane with a dilution of 1:2000 for 2 h at 4 °C. After incubation, the protein band was visualized by adding H_2O_2 and 3, 3'-Diaminobenzidine (DAB) [23].

Experimental design and optimizing cultural conditions

In current study, 20 experiments were designed using Design-Expert software version 13. To optimize the expression of NA in *E. coli* BL21 (DE3) host, the three factors of temperature, induction time, and concentration of IPTG were investigated. Experiments were conducted in the temperature range of 22 to 38 °C, IPTG concentration in the range of 0.1-1.0 mM, and induction time of 1 to 5 h using the Central Composite Design method as indicated in Table 1 (via five replicated center points). A single clone was inoculated into 5 mL of LB medium supplemented with (50 µg/mL kanamycin), and incubated for 16 h at 37 °C/180 rpm. After an optical density of 1.6 was reached at 600 nm (OD_{600}), 100 µL of seed cultures were added to 5 mL of LB media, then incubated at different temperatures (22, 25, 30, 35, and 38 °C) after induction with designed concentrations of IPTG (IPTG was added at OD_{600nm} ~ 0.6) at 180 rpm. The expression of NA (as a response) was analyzed semi-quantitatively using the SDS-PAGE technique by Image J software [27].

Validation of model

The model validity was evaluated based on three parameters (induction time, temperature, and the concentration of IPTG) within the design space. To achieve the maximum NA expression level under the defined conditions, a group of six experimental combinations was carried out

Table 1 The designed experiments to optimize the expression of NA enzyme as a response

RUN	Temperature	Induction Time	Concentration of IPTG	Protein Expression
1	30	3	0.6	0.75
2	35	4	0.3	0.47
3	30	5	0.6	0.41
4	30	3	0.6	0.76
5	22	3	0.6	0.40
6	25	2	0.8	0.46
7	30	1	0.6	0.40
8	35	4	0.8	0.47
9	25	2	0.3	0.47
10	30	3	0.6	0.70
11	30	3	0.6	0.70
12	35	2	0.3	0.43
13	30	3	0.1	0.47
14	25	4	0.3	0.40
15	30	3	0.6	0.73
16	35	2	0.8	0.34
17	38	3	0.6	0.34
18	25	4	0.8	0.50
19	30	3	0.6	0.72
20	30	3	1.0	0.50

in triplicate, and the results of experimental assays were then compared with the predicted values [28, 31].

Purification of optimized NA

Following the expression of optimized NA (250 mL volume), the pellet was dissolved in 10 mL of the lysis buffer containing 300 mM NaCl, 50 mM $NaH_2PO_4.2H_2O$, and 1 mg/mL lysozyme (pH: 6.5) after 1 h incubation at 4°C. The pellet was lysed by sonication method on ice for 20 min at interval 2 min (80 V, 0.4 A). The bacterial lysate was centrifuged at 14,000 g/ 4 °C for 25 min. The sonication process and centrifugation were repeated 3 times. Finally, the 1 mL of supernatant (SDS-PAGE analysis in Figure S1) was loaded on an equilibrated Ni-NTA resin (Qiagen, USA) at 4 °C for 1.5 h. The resin was washed several times with 6 mL of distilled water and 2mL wash buffer (300 mM NaCl, 50 mM $NaH_2PO_4.2H_2O$, pH 6.5). Then, the resin washed three times in a volume of 1 mL with wash buffer containing 20 mM imidazole, 30 mM imidazole, and 50 mM imidazole. Finally, the NA protein was eluted using an elution buffer containing 100 (1 mL), 200 (1 mL), and 250 (1 mL) mM imidazole [27].

NA enzyme kinetics assessment

NA enzymatic parameters were investigated in a flat-bottom 96-well black plate in reactions containing purified NA enzyme in Tris Buffer (25 mM) with pH 6.5 (optimum pH of NA), Ca^{2+} cofactor (10 mM), and various concentrations of 2′-(4-Methylumbelliferyl)-α-D-N-acetylneuraminic acid substrate (MUNANA) obtained from Sigma Aldrich (0, 50, 100, 200, 400, and 600 μM). The fluorescence intensity from the enzymatic reaction was recorded for 60 min (Time; 0, 1, 5, 10, 15, 20, 25, 30, 35, and 60 min) using excitation and emission wavelengths of 360 nm and 460 nm, respectively. The components of the assay were pre-warmed for 30 min at 37 °C. The fluorescent signal value recorded from reactions without NA and the fluorescence signals of Tris Buffer containing calcium chloride were measured as negative control. Also, the fluorescence intensity caused by *Vibrio Cholera* NA (commercial NA: Sigma Aldrich) was recorded as a positive control. Activity and specific activity were calculated based on a 4-methylumbelliferone (4-MU) standard plot (Fluorescent intensity & the concentration of 4-MU(μM)) in Figure S2 [1, 14, 32].

Moreover, to determine the Km values for the NA, fluorescence intensity was monitored at 37 °C for 60 min at the final concentration of 0-600 μM of the MUNANA substrate [32].

NA inhibition with Oseltamivir

The inhibition value of purified NA for Oseltamivir (at 50 nM concentration) was recorded with measuring fluorescent signals at compared to *Vibrio Cholera* NA (commercial NA: Sigma Aldrich). Briefly, the enzyme reactions were performed at a 96-well plate containing purified NA enzyme in Tris Buffer (25 mM) with pH 6.5 (optimum pH of NA), Ca^{2+} cofactor (10 mM), with increasing concentrations of MUNANA-containing substrate buffer (0, 50, 100, 200, 400, and 600 μM) for 60 min at 37 °C [1].

Statistical analysis

The optimization of NA expression at *E. coli* BL21 (DE3) was performed by obtained models from design expert 13 software (https://www.hearne.software/Software/Design-Expert/FreeTrials). The NA expression levels as a response were measured using the second-order polynomial equation. The effect of independent parameters was investigated on the response (expression rate of NA) through a variance analysis (ANOVA) with a p-value of <0.05 that illustrated the significance level. F-test was utilized to investigate the significance of the model equation. Adjusted R^2, predicted R^2, correlation coefficient (R^2), and adequate precision were used to evaluate the quality of the model and its fit. Also, the relationships and interactions between the variables and the response were demonstrated through contour surface plots. Data was analyzed and interpreted using Graph Pad Prism 9.0.0 software (https://www.graphpad.com/updates/prism-900-release-notes).

Results

Expression analysis of NA by SDS-PAGE and Western blot

To screen the best expression host among *E. coli* Bl21 (DE3), ShuffelT7, and SILEX systems for optimization of the culture conditions of NA using statistical experimental design, the NA expression was investigated at two temperatures of 29 °C and 37 °C, three different concentrations of IPTG (0.1, 0.5, and 1 mM) and induction time of 2, 3, 4, and 16 h. The results of SDS-PAGE in Figure S3 and S4 showed that the highest amount of protein expression was on 12% SDS-PAGE gel at 29 °C, 0.5 mM concentration of IPTG, and 3 h after induction at *E. coli* BL21 (DE3) (6.1 µg/mL at molecular weights of 48 kDa) based on the results of Image J. Therefore, the *E. coli* Bl21 (DE3) host was chosen as a suitable host for further optimization of the culture conditions by statistical experimental design. Figure 1 showed the expression of truncated form of NA enzyme at 5 mL cultures at 30 °C, 0.5 mM concentration, and 3 h after induction. The stained gel showed that the NA enzyme was expressed at molecular weights of 48 kDa (Fig. 1a). Moreover, the NA expression was also confirmed by western blot technique (Fig. 1b).

Optimization of NA expression level by statistical experimental design parameters

In this study, CCD was applied for modeling and optimization of NA expression at *E. coli* BL21 (DE3) host due to the model could predict parameters even at their borderline regions. The NA expression levels were optimized based on influential parameters (independent) of temperature, the concentration of IPTG, and induction time by measuring the intensity of protein bands on SDS-PAGE gel [33]. Table 2 showed ANOVA analysis to optimize the expression level of the NA enzyme in *E. coli* Bl21 (DE3) host by Image J software. The results demonstrate that all factors considerably affect the expression level of NA enzyme ($P<0.05$), and the optimal conditions for NA enzyme expression are IPTG concentration of 0.6 mM,

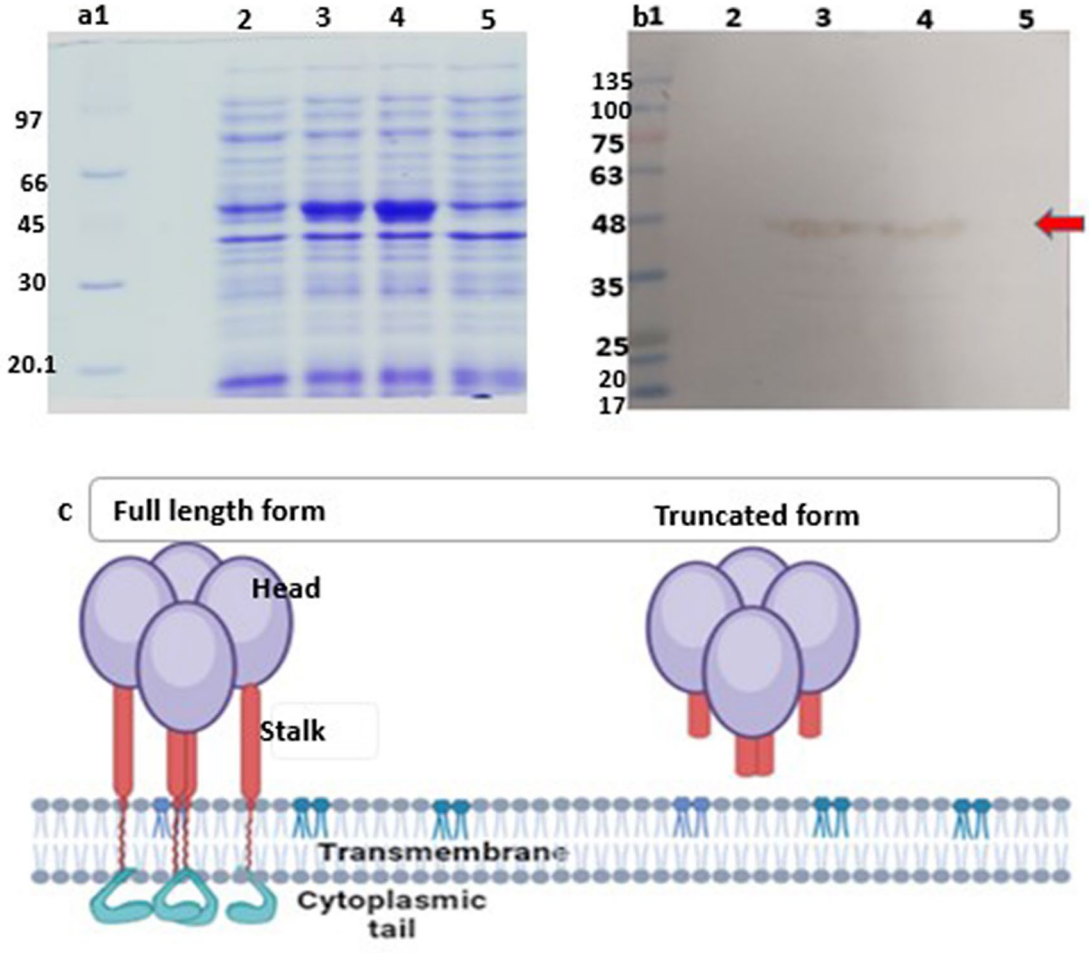

Fig. 1 NA expression analysis. (**a**) SDS PAGE analysis of NA [well 1: protein marker, well 2: NA enzyme expressed before the induction process, wells 3, 4 and 5: 2 h, 3 h and 16 h after induction, respectively]. (**b**) Western blot of NA [Well 1: protein marker, well 2: NA enzyme expressed before the induction process, wells 3 and 4: purified NA. (**c**) Tetramer structure of NA. Full-length form: Each monomer consists of four domains; head, stalk, transmembrane region, and cytoplasmic tail. Truncated form: each monomer consists of a domain head and part of a stalk

Table 2 ANOVA analysis of NA expression at *E. Coli* BL21 (DE3) by the second-order polynomial model

Source	Sum of Squares	df	Mean Square	F-Value	*P*-Value	
Model	0.3924	9	0.0436	45.57	< 0.0001	Significant
A-Temperature	0.0036	1	0.0036	3.73	< 0.05	
B-Induction Time	0.0018	1	0.0018	16.08	< 0.05	
C-Concentration of IPTG	0.0002	1	0.0002	26.99	< 0.05	
AB	0.0050	1	0.0050	5.23	0.0453	
AC	0.0040	1	0.0040	4.23	0.0667	
BC	0.0050	1	0.0050	5.23	0.0453	
A^2	0.1987	1	0.1987	207.68	< 0.0001	
B^2	0.1590	1	0.1590	166.22	< 0.0001	
C^2	0.0849	1	0.0849	88.76	< 0.0001	
Residual	0.0096	10	0.0010			
Lack of Fit	0.0064	5	0.0013	2.05	0.2242	not significant
Pure Error	0.0031	5	0.0986	0.0006		
Cor Total	0.4020	19				

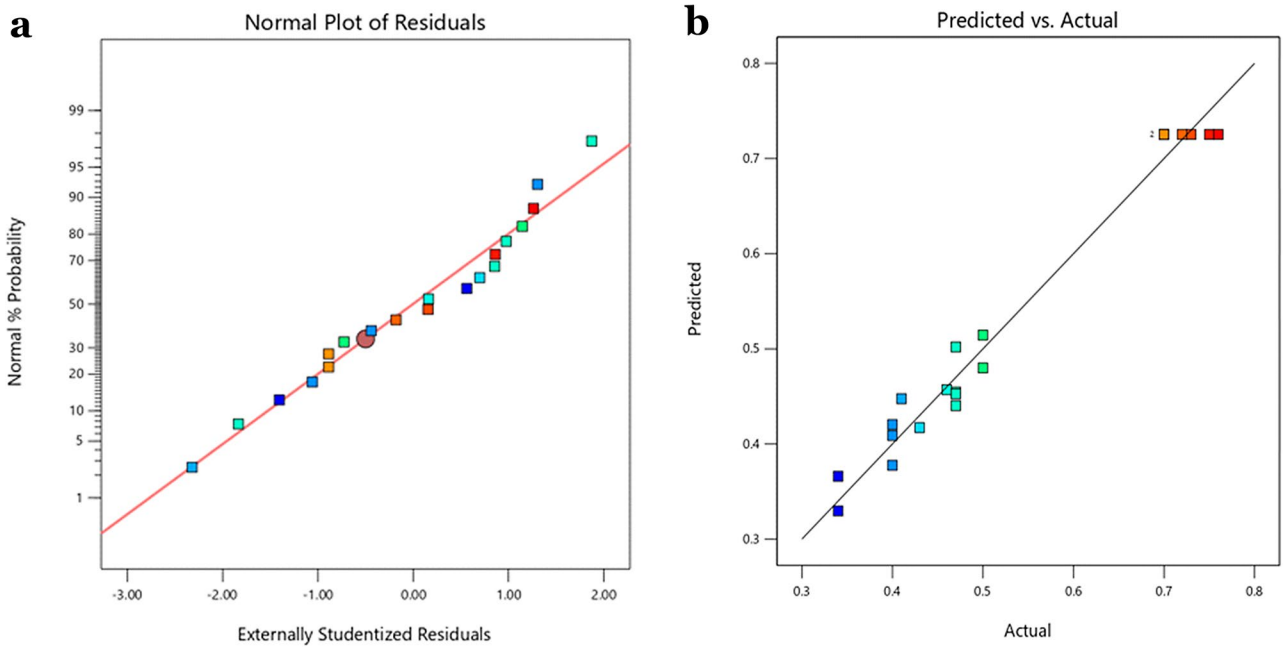

Fig. 2 Normal probability graphs & the plot of actual and predicted values. The plots (**a** and **b**) indicated the relationship between the actual and predicted values of NA expression as a response. The fitting of the model to the empirical data, verified by the closeness of scattered data to the diagonal line

temperature of 30 °C, and expression time of 3 h. The value of Lack of fit showed the deficiency of the model to fit the experimental data, if the lack of fit is significant, the model is removed [28]. The F-value (F: 45.57) of the model was acquired from the ratio of the mean square of the model to the mean square of the residuals. Thus, a non-significant result of lack of fit in this study shows that the (Quadratic) model is correctly fitted.

The values of adjusted R^2 (0.95) were in rational agreement with acquired values predicted R^2 (0.86), and their differences were less than 0.2 Adequate precision indicates the signal- to-noise proportion, and the adequacy of the model verified high values of adequate precision (values > 4 are acceptable). The fitness of the models was further evaluated using a plot of normal probability for the residual to find outlier data and restrictions. The acquired result of the relationship between the actual and predicted values and normal probability graphs (Fig. 2a and b) demonstrated a relatively linear pattern with errors distributed normally; however, a non-linear pattern shows non-normality [28, 34–36].

The effects of independent variables on NA expression levels were indicated in the perturbation graph (Fig. 3). As depicted in Fig. 3, (A) temperature, (B) induction time, and (C) concentration of IPTG of samples had positive contributions at NA expression levels of temperature 22 to 30 °C, induction time 1 to 3 h, and concentration of IPTG 0.1 to 0.6 mM. The interactions of factors

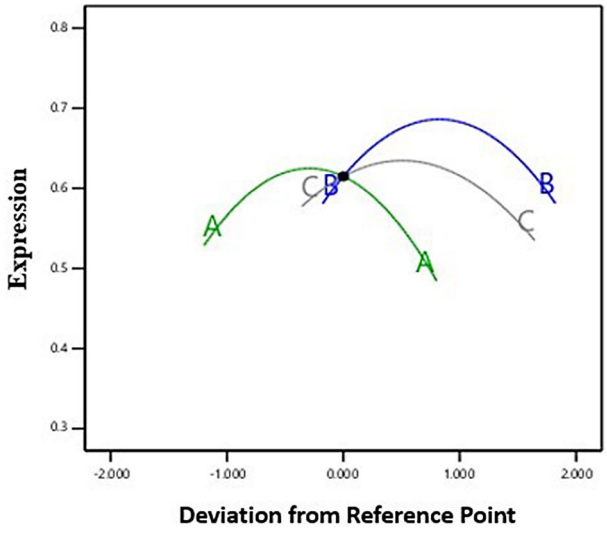

Fig. 3 Perturbation plot. The plots show individual effects of factors (temperature (**A**), induction time (**B**), and concentration of IPTG (**C**) at the deviation of the optimum point (center point) of the plot

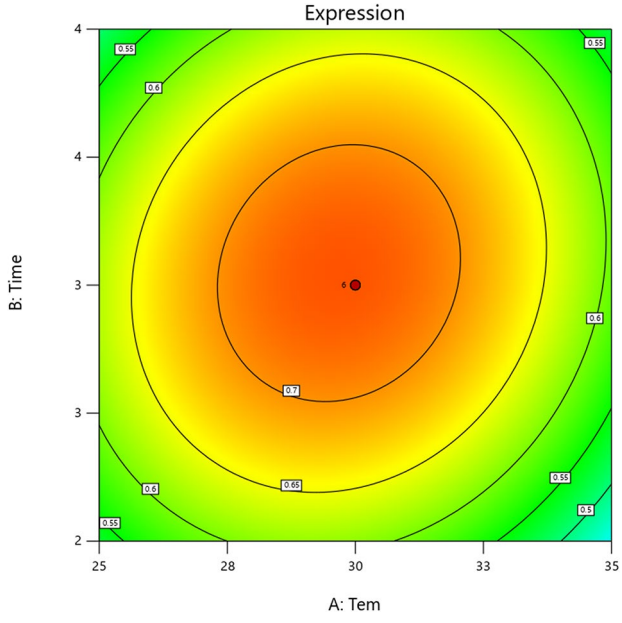

Fig. 4 The effect of temperature (**A**), induction time (**B**), and concentration of IPTG (**C**) on NA expression level

Table 3 Illustrates the kinetic parameters of purified NA for 20 min. Kinetic properties of NA

Sample	NA MUNANA substrate	Positive Control
Activity (IU)	3.5	
Specific Activity (3.5 IU/mg)	~3.5 IU/mg	~4I U/mg
K_m Value (μM)	86.49 ± 0.1	

in curvature contour lines (Fig. 4) were significant. The temperature (30 °C), induction time (3 h), and concentration of IPTG (0.06) were predicted as the optimal criteria resulting in maximum NA expression (7.6 μg/mL) that was measured by Image J (Table 3).

Purification of optimized NA

The purification of NA was analyzed by applying 12% SDS-PAGE gel at 250 mL culture at 30 °C, 0.6 mM concentration, and 3 h after induction. The stained gels confirm the purity of the NA enzyme at molecular weights of 48 kDa and 51 kDa under non-reducing condition (Fig. 5).

The final yield is ~5.7 mg/L of NA in one liter of bacterial culture.

Validation test for optimization factors by T-test analysis

A validation experiment was performed to confirm the application of the optimal conditions at enhancing NA expression level. Thus, in this study, the maximum expression of NA was considered an optimization goal. Six replicated experimental assays were conducted at the best-predicted condition for validating the optimized parameters. To compare predicted values using statistical approach with correspondence the experimental values, one-sample T-test was applied. The p-values (<0.0001) of T-tests confirmed a good relationship between experimental and predicted results [28, 34, 35]. The validation of predicted and experimental NA expression yielded 7.2 ± 0.00 and 7.6 ± 0.11 μg/mL of the enzyme under optimized culture conditions, respectively. As a result, ~2.2-fold rise in overall NA production was achieved compared to the non-optimized conditions.

Enzyme activity assay of NA

Following protein purification, the biological activity of NA was evaluated by measuring fluorescent intensity (in triplicate) resulting from cleaving a fluorogenic 2′-(4-Methylumbelliferyl)-α-D-N-acetylneuraminic acid substrate (MUNANA). The enzyme reaction was triggered by adding substrate at concentrations; 0, 50, 100, 200, 400, and 600 μM. In general, a unit of enzyme (IU) refers to the amount of enzyme for converting one micromole (μmol) of substrate per minute, and typically utilized to illustrate enzyme catalytic activity. The result depicts that the activity of purified NA expressed at *E. coli* BL21 (DE3) (after 3 h incubation at 25 °C/180 rpm for LB medium) is ~3.5 IU (Fig. 6). In the presence of excess MUNANA (600 μM final concentration), The specific activity of purified NA was measured to prevent substrate depletion. The specific activity of the purified NA is >3.5 IU/mg (as measured under the described conditions) close to specific activity of *Vibrio Cholera* NA (Sigma Aldrich, positive control) with 4 IU/mg value.

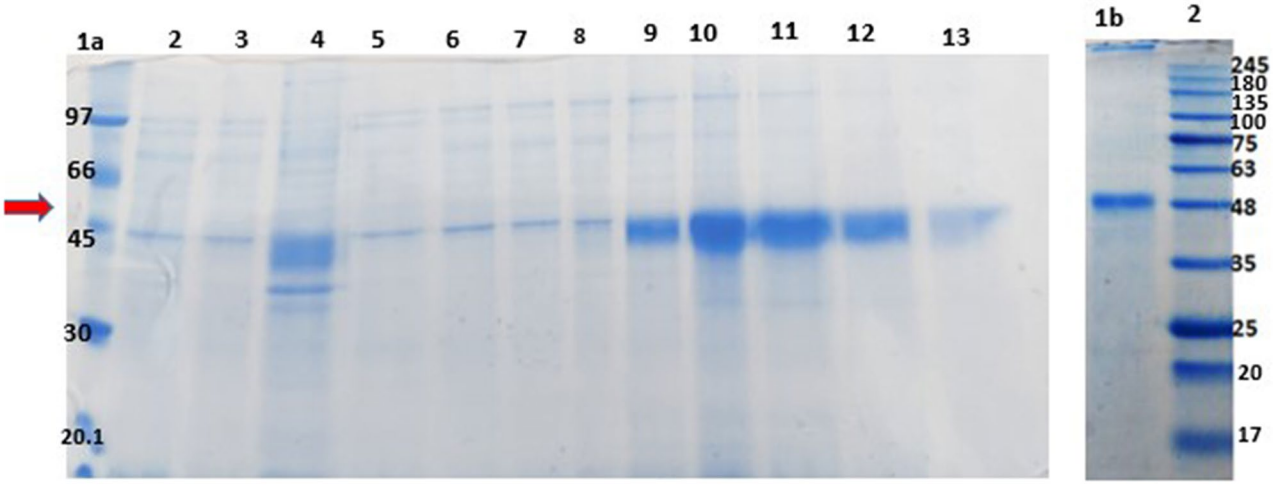

Fig. 5 Analysis of NA purity using SDS-PAGE. (**a**) Well 1: protein marker, wells 2 and 3: purified fraction with wash buffer, wells 4 and 5: purified fraction with 30 mM imidazole, wells 6 and 7: purified fraction with 50 mM imidazole, wells 8 and 9: purified fraction with 100 mM imidazole molar, wells: 10 and 11: imidazole 200 mM, wells: 12 and 13: fraction 250 mM. (**b**) Well 1: 3 h after induction in *E. coli* BL21 (DE3) host at 30 °C and 0.6 mM inducer under non-reducing condition, well 2: protein marker

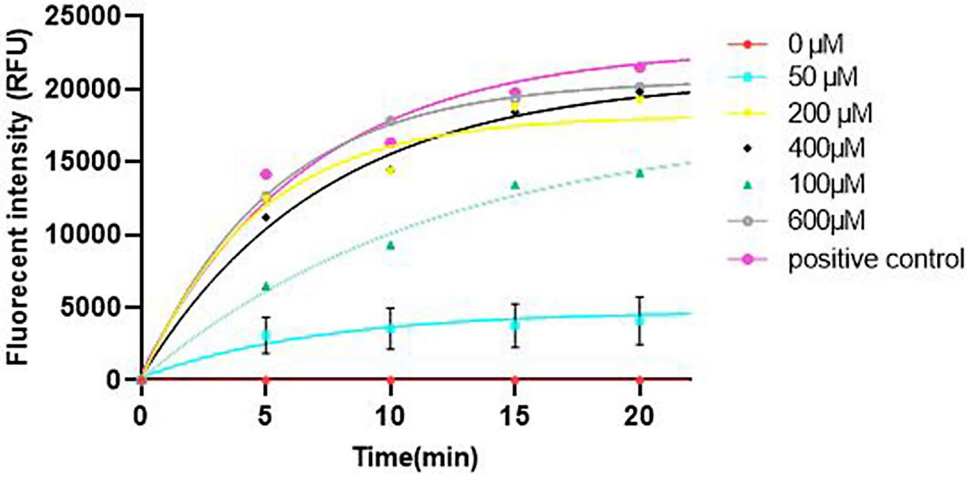

Fig. 6 Determination of specific activity. Figure shows the fluorescence intensity of the different concentrations of the MUNANA substrate (0-600 µM) and *Vibrio Cholera* (as positive control) at 37 °C for 20 min. Fluorescence intensity of Blank signal value (sample without NA) was subtracted from RFU acquired in catalyze of the MUNANA substrate by the recombinant NA (Data represents mean ± SEM)

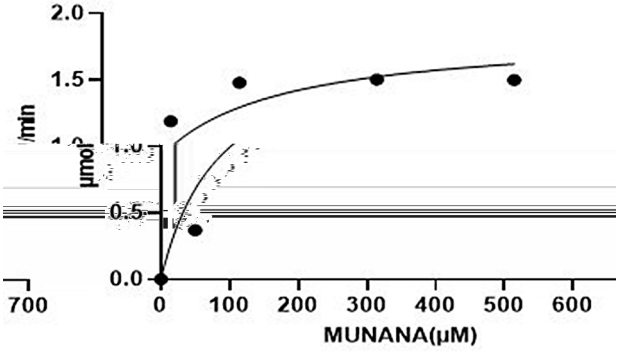

Fig. 7 Measuring of Km for MUNANA substrate. To acquire the Km value for MUNANA, the purified enzyme was incubated with increasing concentration of substrate. Data represents mean ± SEM

To assess the Km values for the purified NA, the enzymes were incubated with enhancing concentrations of MUNANA for 60 min at 37 °C. Km values (86.49 ± 0.1 µM) for MUNANA was determined using the non-linear regression (Fig. 7).

The NA inhibition assay

The result demonstrated that the rate of NA inhibition with Oseltamivir in purified NA and *Vibrio Cholera* NA (commercial NA: Sigma Aldrich) is comparable. In this study, the fluorescent signal resulting from the incubation of the MUNANA substrate with purified NA and *Vibrio Cholera* NA without encountering an NA inhibitor was considered a control in this test. After incubation NA

with Oseltamivir (as a NA inhibitor), the decreasing of affinity of NA to MUNANA substrate was also observed in Fig. 8, which is in accordance with previous studies [1]. The inhibition of NA activity with Oseltamivir suggesting that purified NA have appropriate specificity, and are enzymatically active.

Discussion

It is evident that seasonal influenza lead to a worldwide death of approximately more than 250,000 per year. The studies demonstrated that the existence of vaccines and antiviral therapies have decreased the public anxiety about this viral disease [1, 14]. In light of these incidents, understanding the mechanism of resistance, the development, and improvement of new antiviral drugs are important for the effective control of influenza [37]. These purposes would be extensively obtained by the production of larger amounts of active NA with a high purity and efficiency that is produced at a low cost by a bacterial host.

The NA is a membrane tetramer enzyme with frequent disulfide bonds and glycosylation site. As a result, the expression of the recombinant form of this enzyme in bacterial hosts as a suitable expression host has received less attention [20]. To overcome this restriction, in this study, the NA sequence of different viral subtypes and their post-translation modification were evaluated from the UniProt database. The results illustrated that the glycosylation site is not present in all viral subtypes. It is inferred that this site hasn't a significant role in the activity of the NA enzyme, which is in agreement with previous studies by researchers [38, 39]. Moreover, a truncated form of the enzyme was designed to prevent inappropriate folding, aggregation, and also facilitate the purification process of membrane enzymes. The results of bioinformatics studies from Uniprot database for NA sequence of different strains H1N1 showed that the active site of enzyme exists in the head part of the enzyme [40]. The cytoplasmic tail and the transmembrane domain of NA play a vital role in crucial viral functions. The both of parts provide signals for translocation from the endoplasmic reticulum to the apical surface (that is in association with lipid rafts) [40]. Previous studies indicated that the stalk sequence of the NA enzyme improves the stability of the enzyme. The cysteine residue (s) of the stalk domain can reinforce stabilization of tetramer by forming disulfide bonds between each monomeric unit of NA enzyme [24, 25]. For example; in a study conducted by Castrucci and et al., the result showed that the modification of stalk reported a negative impact on the catalytic rate of enzyme [41, 42]. The other study showed that the placement of the tag sequence in close range to the head site of the NA had an effective destabilizing effect on stability of the tetrameric structure of NA [1]. In contrast, some studies demonstrate that the insertion of the affinity dose not effect on the enzyme activity [14, 43, 44]. Thus, in this study, the expression of truncated form of NA (removing of the tail domain, a transmembrane domain, and part of stalk) was investigated in *E. coli* BL21 (DE3), ShuffelT7, and self-inducible SILEX systems. Enzyme expression screening in three different expression systems) with different temperatures (29 and 37 °C), duration of induction (2, 3, 4, and 16 h), and concentration of inducer (0.1, 0.5, 1 mM) (showed that the yield of the enzyme is higher at 29 °C, 0.5 mM of IPTG, and induction time of 3 h. In addition, the yield of NA enzyme in *E. coli* BL21 (DE3) is higher than other expression systems (Shuffle T7 and SILEX systems) at 29 °C. In agreement with our previous report, SILEX systems at 37 °C have higher expression of recombinant proteins than at lower temperatures. However, the expression of NA enzyme decreases at higher temperature (37 °C).

To achieve the highest level of NA expression in the *E. coli* BL21 (DE3) host, RSM is considered as an effective

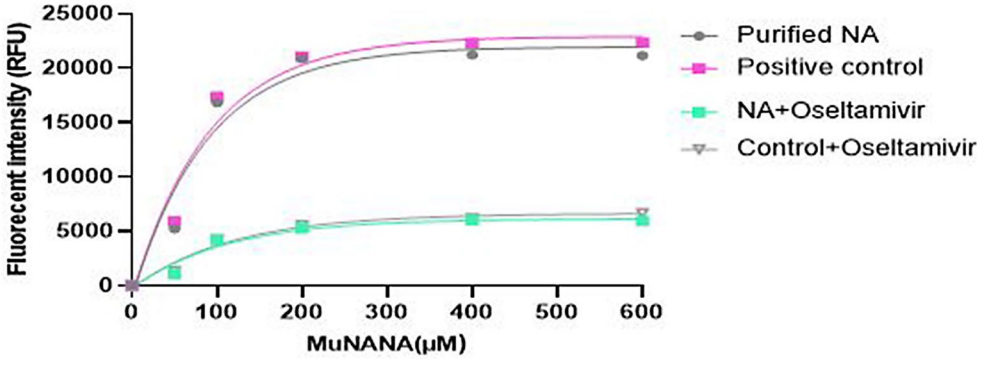

Fig. 8 Determination of NA inhibition by oseltamivir. Figure showed fluorescence intensity of the different concentrations of the MUNANA substrate (0-600 μM) at time: 35 min for purified NA and *Vibrio Cholera* (as positive control). To validate that purified NA and positive control demonstrate similar inhibition values, enzymes incubated with oseltamivir (concentration: 50 nM) at different concentrations of MUNANA substrate. Data represents mean ± SEM in triplicate

and scientific method to optimize cultivation conditions with evaluation of the effects of the parameters on expression level [45, 46]. The type of experimental design in this system is selected according to the number of factors (temperature, concentration of IPTG, and induction time) obtained from previous studies on expression systems [28, 47]. The suitability of the predicted models was investigated based on analysis of variances. The results of tests with a F-value of 45.57 and a p-value < 0.0001 confirm the significance of the model. As summarized in Table 2, the maximum amount of produced NA was obtained (by measuring protein bands with ImageJ software) in run 4 (7.6 μg/mL), while the lowest value was observed in runs 16 and 17 (3.4 μg/mL). The results were assessed by a second-order polynomial equation as expressed below [23, 48].

$$y = \alpha 0 + \sum_{i=1}^{n} \alpha i X i + \sum_{i=1}^{n} \alpha i i X i 2 + \sum_{i=1}^{n} \sum_{j=i+1}^{n} \alpha i j X i X j$$

Our findings showed that the expression of a truncated form of NA in *E. coli* BL21 (DE3) can be a promising approach at optimizing conditions including; temperature of 30 °C, induction time of 3 h, and 0.6 mM concentration of IPTG. The negative distribution of parameters from the temperature (at 30–37 °C) can be ascribed to more bacterial cells growth due to enhanced temperature [49]. In another study which is performed by Vera et al., a large amount of recombinant proteins is aggregated with rising temperature of 15–37 °C. It might be due to the fact that at lower temperatures, the bacterial systems providing sufficient time for the expression of new recombinant proteins, and transcription to accurate folding [50, 51]. It is inferred that low temperature can increase the efficiency of soluble protein production and plasmid stability [52]. The our result showed that temperature 30 °C could considerably improve the expression of the NA compared to with the ordinary growth temperature of *E. coli* BL21 (DE3) at 37 °C. Also, the appropriate time for induction can affect the protein expression rate. Our data are in agreement with the finding of a previous study, that the higher expression and protein stability of enzyme gained in a lower induction time [53, 54].

The optimal criteria of NA expression in *E. coli* BL21 (DE3) was predicted as temperature (30 °C), induction time (3 h), and concentration of IPTG (0.06). After purification of NA, the activity of each active and soluble monomer of non-glycosylated NA was verified by using fluorimetric activity assays with an increasing substrate concentration of 0 to 600 μM [1, 32]. Figure 6a depicted the enhancement of fluorescent product during time for different substrate concentrations for 35 min based on 4-Methylumbelliferone (MU) standard. With increasing time, the upward trend of fluorescence intensity decreases somewhat. This issue can be due to changes in the pH of the enzyme environment, and or temperature fluctuations during fluorescence intensity measurement at different times [32]. The studies demonstrate that the optimal activity of this enzyme arises at a pH range of 5.5–6.5, and the existence of Ca^{2+} (as a cofactor) considered to be vital during the enzyme reaction for both thermostability and enzyme activity of the NA [39]. In this research, the specific activity; ~3.5 IU/mg (using MUNANA substrate) were calculated for purified NA. The result showed that the activity level of our NA per milligram of protein (Specific activity) is comparable to the commercial form (*Vibrio Cholera* with specific activity; ~1–4 IU /mg, Sigma Aldrich). Moreover, the activity level of the purified NA is somewhat equal to or higher than the commercial forms of NA enzyme as; (i) recombinant H1N1 NA expressed at *Spodoptera frugiperda* with specific activity; >2,500 pmol/min/μg (Cat NO; 4858-NM), (ii) *Vibrio Cholera* NA with specific activity; 1–5 IU/mg (Sigma, N7885), (iii) *Clostridium perfringens* NA with specific activity; 3.5-8 IU/mg (CAS NO; 9001-67-6), and (iv) recombinant H1N1 NA expressed at Baculovirus-Insect Cell (the value of specific activity not reported, Cat No;40568-V08B). However, the interpretation of enzyme activity results among different laboratories cannot be sufficiently reliable, due to the measurement of fluorescence intensity is performed with different devices and different measurement protocols [14, 55]. The Km value for the recombinant NA was 86.49 ± 0.1 μM, and this criteria determined by incubating the NA with varying concentrations of MUNANA [32]. In a study by Campbell et al., the expression of H1N1 NA was reported (> 3000 EU/mL) in the eukaryotic host HEK293-6E [14]. At a study performed by Yongkiettrakul et al. in yeast host, the expressed NA has specific activity similar to NA of H1N1, H5N1, and H1N3 virus. However this NA has high molecular weight compared with the NA virus due to hyper glycosylation [17]. Moreover, the expression of NA in tobacco plants leads to an insoluble product [16, 17]. The expression systems based on baculovirus/insect cell produce active NA, although, the survival and maintenance of these expression systems faces limitations [19, 56, 57].

Conclusions

The high quality and proper functional activity of the truncated neuraminidase described in this research show that *E. coli* can be a suitable host for a wide range of applications with less cost and risk compared to eukaryotic expression systems.

Abbreviations

SILEX	Self-induced expression system
RFU	Relative fluorescent unit
RSM	Response surface methodology

CCD central composite design
RSD Relative standard deviation
SOP Super Optimal Broth LB: Luria-Bertani

Supplementary Information

The online version contains supplementary material available at https://doi.org/10.1186/s12934-024-02587-8.

Supplementary Material 1

Acknowledgements
The project was financially supported by Pasteur Institute of Iran. The authors wish to express their deep gratitude to all who provided support during the course.

Author contributions
F. F, K. A, B. F, F. S. S designed the study. F. S. S., Z. B conducted the experiments and drafted the manuscript. K. A, F. F, B. F, F. S. S analyzed and interpreted the results. All authors reviewed and approved the final version of the manuscript.

Funding
This work was supported by Pasteur Institute of Iran (grant # 2106).

Data availability
No datasets were generated or analysed during the current study.

Declarations

Ethics approval and consent to participate
Not applicable.

Consent for publication
Not applicable.

Competing interests
The authors declare no competing interests.

Author details
[1]Department of Influenza and Respiratory Viruses, Pasteur Institute of Iran, Tehran, Iran
[2]Virology Department, Pasteur Institute of Iran, Tehran, Iran

Received: 17 July 2024 / Accepted: 9 November 2024
Published online: 25 November 2024

References

1. Schmidt PM, Attwood RM, Mohr PG, Barrett SA, McKimm-Breschkin JL. A generic system for the expression and purification of soluble and stable influenza neuraminidase. PLoS ONE. 2011;6:e16284.
2. Crusat M, De Jong MD. Neuraminidase inhibitors and their role in avian and pandemic influenza. Antivir Ther. 2007;12:593–602.
3. Pleschka S. Overview of influenza viruses. Swine Influenza 2012:1–20.
4. Hayden FG, Atmar RL, Schilling M, Johnson C, Poretz D, Paar D, Huson L, Ward P, Mills RG, Group OS. Use of the selective oral neuraminidase inhibitor oseltamivir to prevent influenza. N Engl J Med. 1999;341:1336–43.
5. McAuley JL, Gilbertson BP, Trifkovic S, Brown LE, McKimm-Breschkin JL. Influenza virus neuraminidase structure and functions. Front Microbiol. 2019;10:39.
6. Bloom JD, Gong LI, Baltimore D. Permissive secondary mutations enable the evolution of influenza oseltamivir resistance. Science. 2010;328:1272–5.
7. Collins P, Haire L, Lin Y, Liu J, Russell R, Walker P, Martin S, Daniels R, Gregory V, Skehel J. Structural basis for oseltamivir resistance of influenza viruses. Vaccine. 2009;27:6317–23.
8. Collins PJ, Haire LF, Lin YP, Liu J, Russell RJ, Walker PA, Skehel JJ, Martin SR, Hay AJ, Gamblin SJ. Crystal structures of oseltamivir-resistant influenza virus neuraminidase mutants. Nature. 2008;453:1258–61.
9. McNicholl IR, McNicholl JJ. Neuraminidase inhibitors: zanamivir and oseltamivir. Ann Pharmacother. 2001;35:57–70.
10. Air GM, Laver WG. The neuraminidase of influenza virus. Proteins Struct Funct Bioinform. 1989;6:341–56.
11. Varghese J, Laver W, Colman PM. Structure of the influenza virus glycoprotein antigen neuraminidase at 2.9 Å resolution. Nature. 1983;303:35–40.
12. McKimm-Breschkin JL, Caldwell JB, Guthrie RE, Kortt AA. A new method for the purification of the influenza a virus neuraminidase. J Virol Methods. 1991;32:121–4.
13. Taubenberger JK, Reid AH, Fanning TG. The 1918 influenza virus: a killer comes into view. Virology. 2000;274:241–5.
14. Campbell AC, Tanner JJ, Krause KL. Optimisation of Neuraminidase expression for Use in Drug Discovery by using HEK293-6E cells. Viruses. 2021;13:1893.
15. Ecker JW, Kirchenbaum GA, Pierce SR, Skarlupka AL, Abreu RB, Cooper RE, Taylor-Mulneix D, Ross TM, Sautto GA. High-yield expression and purification of recombinant influenza virus proteins from stably-transfected mammalian cell lines. Vaccines. 2020;8:462.
16. Martinet W, Saelens X, Deroo T, Neirynck S, Contreras R, Min Jou W, Fiers W. Protection of mice against a lethal influenza challenge by immunization with yeast-derived recombinant influenza neuraminidase. Eur J Biochem. 1997;247:332–8.
17. Yongkiettrakul S, Boonyapakron K, Jongkaewwattana A, Wanitchang A, Leartsakulpanich U, Chitnumsub P, Eurwilaichitr L, Yuthavong Y. Avian influenza A/H5N1 neuraminidase expressed in yeast with a functional head domain. J Virol Methods. 2009;156:44–51.
18. Deroo T, Jou WM, Fiers W. Recombinant neuraminidase vaccine protects against lethal influenza. Vaccine. 1996;14:561–9.
19. Mather KA, White JF, Hudson PJ, McKimm-Breschkin JL. Expression of influenza neuraminidase in baculovirus-infected cells. Virus Res. 1992;26:127–39.
20. Lipničanová S, Chmelová D, Godány A, Ondrejovič M, Miertuš S. Purification of viral neuraminidase from inclusion bodies produced by recombinant Escherichia coli. J Biotechnol. 2020;316:27–34.
21. Shariati FS, Keramati M, Valizadeh V, Cohan RA, Norouzian D. Comparison of E. Coli based self-inducible expression systems containing different human heat shock proteins. Sci Rep. 2021;11:4576.
22. Shariati FS, Norouzian D, Valizadeh V, Ahangari Cohan R, Keramati M. Rapid screening of high expressing Escherichia coli colonies using a novel dicistronic-autoinducible system. Microb Cell Fact. 2021;20:1–11.
23. Shariati FS, Keramati M, Cohan RA. Indirect optimization of staphylokinase expression level in dicistronic auto-inducible system. AMB Express. 2022;12:1–8.
24. Creytens S, Pascha MN, Ballegeer M, Saelens X, de Haan CA. Influenza neuraminidase characteristics and potential as a vaccine target. Front Immunol. 2021;12:786617.
25. Shtyrya Y, Mochalova L, Bovin N. Influenza virus neuraminidase: structure and function. Acta Naturae (англоязычная версия). 2009;1:26–32.
26. Robinson M-P, Jung J, Lopez-Barbosa N, Chang M, Li M, Jaroentomeechai T, Cox EC, Zheng X, Berkmen M, DeLisa MP. Isolation of full-length IgG antibodies from combinatorial libraries expressed in the cytoplasm of Escherichia coli. Nat Commun. 2023;14:3514.
27. Sam S, Ofoghi H, Farahmand B. Developing of SARS-CoV-2 fusion protein expressed in E. Coli Shuffle T7 for enhanced ELISA detection sensitivity–an integrated experimental and bioinformatic approach. J Biomol Struct Dynamics 2024:1–16.
28. Shariati FS, Keramati M, Cohan RA. Indirect optimization of staphylokinase expression level in dicistronic auto-inducible system. AMB Express. 2022;12:124.
29. Njoku CN, Otisi SK. Application of central composite design with design expert v13 in process optimization. Response surface methodology-research advances and applications. IntechOpen; 2023.
30. Kurdi SS, M-Ridha MJ. Determination of the optimum conditions for urease extraction from Chickpea seeds using (Design Expert Software). Al-Khwarizmi Eng J. 2024;20:87–96.
31. Bhardwaj KK, Kumar R, Bhagta S, Gupta R. Optimization of culture conditions by response surface methodology for production of extracellular esterase from Serratia sp. EST-4. J King Saud University-Science. 2021;33:101603.
32. Marathe BM, Leveˆque V, Klumpp K, Webster RG, Govorkova EA. Determination of neuraminidase kinetic constants using whole influenza virus preparations and correction for spectroscopic interference by a fluorogenic substrate. PLoS ONE. 2013;8:e71401.

33. Bhattacharya S. Central composite design for response surface methodology and its application in pharmacy. Response surface methodology in engineering science. IntechOpen; 2021.
34. Pal D, Patel G, Dobariya P, Nile SH, Pande AH, Banerjee UC. Optimization of medium composition to increase the expression of recombinant human interferon-β using the plackett–Burman and central composite design in E. Coli SE1. 3 Biotech. 2021;11:226.
35. Bayuo J, Abukari MA, Pelig-Ba KB. Optimization using central composite design (CCD) of response surface methodology (RSM) for biosorption of hexavalent chromium from aqueous media. Appl Water Sci. 2020;10:1–12.
36. Gomaa FAM, Selim HMRM, Alshahrani MY, Aboshanab KM. Central composite design for optimizing istamycin production by Streptomyces tenjimariensis. World J Microbiol Biotechnol. 2024;40:316.
37. Glanz VY, Myasoedova VA, Grechko AV, Orekhov AN. Inhibition of sialidase activity as a therapeutic approach. Drug Des Devel Ther 2018:3431–7.
38. McAuley JL, Gilbertson BP, Trifkovic S, Brown LE, McKimm-Breschkin JL. Influenza virus neuraminidase structure and functions. Front Microbiol. 2019;10:432609.
39. Gaymard A, Le Briand N, Frobert E, Lina B, Escuret V. Functional balance between neuraminidase and haemagglutinin in influenza viruses. Clin Microbiol Infect. 2016;22:975–83.
40. Kim J-H, Resende R, Wennekes T, Chen H-M, Bance N, Buchini S, Watts AG, Pilling P, Streltsov VA, Petric M. Mechanism-based covalent neuraminidase inhibitors with broad-spectrum influenza antiviral activity. Science. 2013;340:71–5.
41. Castrucci MR, Bilsel P, Kawaoka Y. Attenuation of influenza a virus by insertion of a foreign epitope into the neuraminidase. J Virol. 1992;66:4647–53.
42. Castrucci MR, Kawaoka Y. Biologic importance of neuraminidase stalk length in influenza a virus. J Virol. 1993;67:759–64.
43. Goto H, Bethell RC, Kawaoka Y. Mutations affecting the sensitivity of the influenza virus neuraminidase to 4-guanidino-2, 4-dideoxy-2, 3-dehydro-N-acetylneuraminic acid. Virology. 1997;238:265–72.
44. Zürcher T, Yates PJ, Daly J, Sahasrabudhe A, Walters M, Dash L, Tisdale M, McKimm-Breschkin JL. Mutations conferring zanamivir resistance in human influenza virus N2 neuraminidases compromise virus fitness and are not stably maintained in vitro. J Antimicrob Chemother. 2006;58:723–32.
45. Lipničanová S, Legerská B, Chmelová D, Ondrejovič M, Miertuš S. Optimization of an inclusion body-based production of the influenza virus neuraminidase in Escherichia coli. Biomolecules. 2022;12:331.
46. Sahu R, Meghavarnam AK, Janakiraman S. Response surface methodology: an effective optimization strategy for enhanced production of nitrile hydratase (NHase) by Rhodococcus rhodochrous (RS-6). Heliyon 2020, 6.
47. Akbarzadeh A, Dehnavi E, Aghaeepoor M, Amani J. Optimization of recombinant expression of synthetic bacterial phytase in Pichia pastoris using response surface methodology. Jundishapur J Microbiol 2015, 8.
48. Koivunen ME, Horwath WR. Methylene urea as a slow-release nitrogen source for processing tomatoes. Nutr Cycl Agrosyst. 2005;71:177–90.
49. MacDonald LM, Armson A, Thompson RA, Reynoldson JA. Characterization of factors favoring the expression of soluble protozoan tubulin proteins in *Escherichia coli*. Protein Expr Purif. 2003;29:117–22.
50. Vaz MRF, de Sousa Junior FC, Costa LMR, dos Santos ES, Martins DRA, de Macedo GR. Optimization of culture medium for cell growth and expression of 648 antigen from *Leishmania infantum* chagasi in recombinant *Escherichia coli M15*. Ann Microbiol. 2015;65:1607–13.
51. Vera A, González-Montalbán N, Arís A, Villaverde A. The conformational quality of insoluble recombinant proteins is enhanced at low growth temperatures. Biotechnol Bioeng. 2007;96:1101–6.
52. Hong F, Meinander NQ, Jönsson LJ. Fermentation strategies for improved heterologous expression of laccase in *Pichia pastoris*. Biotechnol Bioeng. 2002;79:438–49.
53. Huang C-J, Peng H-L, Patel AK, Singhania RR, Dong C-D, Cheng C-Y. Effects of lower temperature on expression and biochemical characteristics of hcv ns3 antigen recombinant protein. Catalysts. 2021;11:1297.
54. Schumann W, Ferreira LCS. Production of recombinant proteins in Escherichia coli. Genet Mol Biology. 2004;27:442–53.
55. Prevato M, Ferlenghi I, Bonci A, Uematsu Y, Anselmi G, Giusti F, Bertholet S, Legay F, Telford JL, Settembre EC. Expression and characterization of recombinant, tetrameric and enzymatically active influenza neuraminidase for the setup of an enzyme-linked lectin-based assay. PLoS ONE. 2015;10:e0135474.
56. Margine I, Palese P, Krammer F. Expression of functional recombinant hemagglutinin and neuraminidase proteins from the novel H7N9 influenza virus using the baculovirus expression system. JoVE (Journal Visualized Experiments) 2013:e51112.
57. Grabherr R, Ernst W. Baculovirus for eukaryotic protein display. Curr Gene Ther. 2010;10:195–200.

Publisher's note

Springer Nature remains neutral with regard to jurisdictional claims in published maps and institutional affiliations.